

ELECTRON IRRADIATION OF CARBON DISULFIDE–OXYGEN ICES: TOWARD THE FORMATION OF SULFUR-BEARING MOLECULES IN INTERSTELLAR ICES

SURAJIT MAITY AND RALF I. KAISER

Department of Chemistry, University of Hawai‘i at Manoa, Honolulu, HI 96822, USA
Received 2013 April 23; accepted 2013 July 1; published 2013 August 6

ABSTRACT

The formation of sulfur-bearing molecules in interstellar ices was investigated during the irradiation of carbon disulfide (CS₂)–oxygen (O₂) ices with energetic electrons at 12 K. The irradiation-induced chemical processing of these ices was monitored online and in situ via Fourier transform infrared spectroscopy to probe the newly formed products quantitatively. The sulfur-bearing molecules produced during the irradiation were sulfur dioxide (SO₂), sulfur trioxide (SO₃), and carbonyl sulfide (OCS). Formations of carbon dioxide (CO₂), carbon monoxide (CO), and ozone (O₃) were observed as well. To fit the temporal evolution of the newly formed products and to elucidate the underlying reaction pathways, kinetic reaction schemes were developed and numerical sets of rate constants were derived. Our studies suggest that carbon disulfide (CS₂) can be easily transformed to carbonyl sulfide (OCS) via reactions with suprathreshold atomic oxygen (O), which can be released from oxygen-containing precursors such as water (H₂O), carbon dioxide (CO₂), and/or methanol (CH₃OH) upon interaction with ionizing radiation. This investigation corroborates that carbonyl sulfide (OCS) and sulfur dioxide (SO₂) are the dominant sulfur-bearing molecules in interstellar ices.

Key words: astrochemistry – cosmic rays – ISM: molecules – methods: laboratory – techniques: spectroscopic

Online-only material: color figures

1. INTRODUCTION

During the past decades, the interstellar sulfur chemistry has received considerable attention since the detection of a series of sulfur-containing molecules in the interstellar medium: carbon monosulfide (CS) in Orion A, W51, and IRC+10216 (Penzias et al. 1971), carbonyl sulfide (OCS) in Sgr B2 (Jefferts et al. 1971), hydrogen sulfide (H₂S) toward Orion A and W51, (Thaddeus et al. 1972), sulfur monoxide (SO) in Orion A, W51, and Sgr B2 (Gottlieb & Ball 1973), and sulfur dioxide (SO₂) in Sgr B2 (Snyder et al. 1975). Until now, 15 sulfur-bearing species have been detected in interstellar environments and also in cometary comae (Lovas & Dragoset 2004). The dominant sulfur carriers in the gas phase are sulfur dioxide (SO₂), sulfur monoxide (SO), hydrogen sulfide (H₂S), carbon monosulfide (CS), thioformaldehyde (H₂CS), as well as carbonyl sulfide (OCS; Ferrante et al. 2008). Several chemical gas phase models have been proposed to investigate the sulfur chemistry in these environments (Prasad & Huntress 1982; Oppenheimer & Dalgarno 1974; Doty et al. 2002; Garrod et al. 2007; Millar & Herbst 1990; Wakelam et al. 2011). These models acknowledged that in order to explain the gas phase abundances of sulfur-bearing molecules, the required elemental sulfur abundance should be of the order of 10^{−7} to 10^{−8} relative to hydrogen. However, the cosmic elemental sulfur abundance is about 10^{−5} (Lodders 2003; Sofia et al. 1994; van Steenbergen & Shull 1988). To account for this discrepancy, Garozzo et al. (2010), Palumbo et al. (1997), and Ward et al. (2012) proposed that in dense clouds, a significant amount of sulfur must be locked up in the icy grain mantle.

However, until now, only two sulfur-containing molecules, sulfur dioxide (SO₂) and carbonyl sulfide (OCS), have been identified in interstellar ices (Gibb et al. 2004; Boogert et al. 1997; Palumbo et al. 1995, 1997; Zasowski et al. 2009). The presence of hydrogen sulfide (H₂S) was also proposed via the observation of the 3.90 μm (2564 cm^{−1}) band toward the

embedded protostar W33A (Geballe et al. 1985); however, the assignment of the band remained debatable since it overlaps with the 3.92 μm (2550 cm^{−1}) band of methanol (Garozzo et al. 2010). Recent proton irradiation experiments (200–800 keV) on mixed ices of SO₂ and H₂S with carbon monoxide (CO) resulted in the formation of carbon disulfide (CS₂; Ferrante et al. 2008; Garozzo, et al. 2010). Furthermore, proton irradiation of the OCS ices resulted in the formation of CS₂ as a major reaction product (Ferrante et al. 2008). Based on these experiments, the authors suggested that CS₂ may act as a reservoir of sulfur for the interstellar ices. So far, carbon disulfide has not been detected in interstellar ices, perhaps due to the overlap of its most prominent infrared band at 6.54 μm (1530 cm^{−1}) with the broad absorption features of the C–O stretch of the formate anion (HCOO[−]) at 6.33 μm (1580 cm^{−1}), the H–O–H bend of water (H₂O) at 6.02 μm (1660 cm^{−1}), and/or the O–H bend, and the C–H deformation of interstellar organics at 6.82 μm (1470 cm^{−1}; Gibb et al. 2004; Garozzo et al. 2010). However, carbon disulfide is proposed as the parent molecule (Lovas & Dragoset 2004; Penzias et al. 1971; Williams & Blitz 1998) of carbon monosulfide (CS) as detected in molecular clouds (Williams & Blitz 1998), circumstellar envelopes (Woods et al. 2003), and planetary nebulae (Martin et al. 2005). Furthermore, CS₂ has been detected in circumstellar envelopes (Woods et al. 2003), in comets (Jackson et al. 1982), in Jupiter during the impact of comet Schoemaker-Levy 9 (SL-9; Heynmann et al. 2000), as well as in the atmospheres of Venus and Io (Barker 1979; Jackson et al. 1982).

Based on the fact that both sulfur-containing species identified in interstellar ices (SO₂ and OCS) contain an oxygen atom, experiments were also performed on the reaction between atomic oxygen and carbon disulfide in order to investigate the formation of carbonyl sulfide (OCS) (Ward et al. 2012). Here, atomic oxygen (O) was produced via the microwave discharge of oxygen gas (O₂). The gas mixture was then co-deposited with carbon disulfide (CS₂) on a substrate kept at temperatures

between 15 K to 75 K. This temperature-dependent study revealed that in the presence of oxygen atoms, carbon disulfide (CS_2) readily converted to carbonyl sulfide (OCS; Ward et al. 2012). At a low temperature (15–20 K), the reaction was proposed to proceed via the formation of carbon monosulfide (CS) and sulfur monoxide (SO) intermediates, which eventually reacted with atomic oxygen to form carbonyl sulfide (OCS). The reaction of atomic oxygen and carbon disulfide was also investigated back in 1973 by Jones & Taube. Here, the photolysis of the argon (Ar) matrix (15 K and 30 K) and the xenon (Xe) matrix (60 K) containing carbon disulfide and ozone (O_3) were studied using several conventional light sources, such as mercury lamps (260.0 nm) and cadmium resonance lamps (228.8 nm). The infrared spectroscopic investigations revealed the formations of OCS, SO_2 , and SO_3 as major products with minor amounts of CO. Similar experiments were performed while probing the reaction of CS_2 with atomic oxygen (O) at ~ 13 K (Lo et al. 2004); these studies revealed the formation of carbonyl sulfide (OCS), sulfur dioxide (SO_2), and sulfur trioxide (SO_3) along with carbon monosulfide (CS) and sulfur monoxide (SO). The reaction of CS_2 with atomic oxygen (O) was also investigated in the gas phase. The crossed molecular beam reaction of CS_2 and atomic oxygen (O; ^3P) was studied via a single collision condition at a translational energy of 85 kJ mol^{-1} (Rochford et al. 1995). The quadrupole mass spectroscopic detection revealed the formation of CS and SO as major reaction products under single collision conditions. Furthermore, the reaction of CS_2 with atomic oxygen as produced via photolysis of nitrogen dioxide (NO_2) was studied in a gas phase. Laser induced fluorescence detection (LIF) revealed the formations of CS and SO as major reaction products (Cheng et al. 2001).

However, based on the previous experimental studies, the systematic understanding of the chemistry of sulfur-bearing molecules in interstellar ices is far from complete since the reaction pathways were mainly “guessed” based on chemical intuition, but not derived from kinetic, i.e., temporal profiles, of the reactants and products within the ices. In this report, we present a detailed experimental study on the irradiation-induced reaction of solid carbon disulfide (CS_2)–oxygen (O_2) ices via energetic electrons at low temperature (12 K) with energetic electrons. Note that in nature, carbon disulfide–oxygen ices rarely exist; molecular oxygen was utilized solely as a source of atomic oxygen reacting with carbon disulfide. Here, we will demonstrate not only the production rates of the newly formed species, but also the underlying kinetics and reaction mechanisms based on a simultaneous solution of coupled sets of differential rate equations of the newly formed products monitored online and in situ in an attempt to better understand the sulfur chemistry in interstellar ices.

2. EXPERIMENTAL METHODS

The experiments were carried out in a contamination-free ultra-high vacuum chamber held at a base pressure of 5×10^{-11} Torr (Bennett et al. 2004). A polished silver wafer, interfaced to a two-stage closed-cycle helium refrigerator and a programmable temperature controller, was suspended on a rotary platform and situated in the center of the main chamber. The temperature of the silver crystal can be regulated between 10 K and 330 K with a precision of ± 0.3 K. The ices were prepared by co-condensation of carbon disulfide (CS_2 , Acros Organics, 99.9%) vapor and oxygen gas (O_2 , BOC gases, 99.999%) via two precision leak valves coupled with glass capillary arrays at pressures of up to 2.3×10^{-7} Torr for 15

Table 1
Infrared Absorption Features of the Reactants and Newly Formed Products During the Irradiation of Carbon Disulfide (CS_2)–Oxygen (O_2) Ices at 12 K

Irradiation at 12 K		Literature Assignment			
Before (cm^{-1})	After (cm^{-1})	Ref.	(cm^{-1})	Assignment	Carrier
	2342	1	2342	ν_3	$^{16}\text{O}^{16}\text{O}$
	2324	2	2330	ν_3	$^{16}\text{O}^{18}\text{O}$
	2306	3	2310	ν_3	$^{18}\text{O}^{18}\text{O}$
2158		4, 5	2178	$\nu_1 + \nu_3$	CS_2
	2139	1	2139	ν_1	C^{16}O
	2087	6	2088	ν_1	C^{18}O
	2068	4,7	2079	ν_{10}	C_3S_2
	2039	8	2049	ν_1	^{16}OCS
	2002	9	2025	ν_1	^{18}OCS
1524		4,5	1528	ν_3	CS_2
1461		4,5	1475	ν_3	$^{13}\text{CS}_2$
	1399	8	1400	ν_3	$\text{S}^{16}\text{O}_3; \text{S}^{16}\text{O}_3$
	1388	8,9	1385	ν_3	S^{16}O_3
	1358	11	...	ν_3	$\text{S}^{18}\text{O}_3; \text{S}^{18}\text{O}_3$
	1345	11	1349	ν_3	S^{18}O_3
	1335	8,9	1337	ν_3	$^{16}\text{OS}^{16}\text{O}$
	1312	11	1333	ν_3	$^{16}\text{OS}^{18}\text{O}$
	1290	8	1306	ν_3	$^{18}\text{OS}^{18}\text{O}$
		^a	4,5	1270	CS
	1148	8,9	1150	ν_1	$^{16}\text{OS}^{16}\text{O}$
	1120	11	1122	ν_1	$^{16}\text{OS}^{18}\text{O}$
	1096	8,9	1100	ν_1	$^{18}\text{OS}^{18}\text{O}$
		^b	8	1137	S^{16}O
		^b	8	1092	S^{18}O
	1040	12	1037	ν_3	$^{16}\text{O}_3$
	982	11	983	ν_3	$^{18}\text{O}_3$
	657	1	658	ν_2	$^{16}\text{O}^{16}\text{O}$
	528	8	520	ν_2	$^{16}\text{O}^{16}\text{O}$

Notes.

^a The weak absorption feature of CS (ν_1) submerged with adjacent strong $^{16}\text{OS}^{16}\text{O}$ (ν_3) band.

^b The weak absorption features of S^{16}O (ν_1) and S^{18}O (ν_1) submerged with adjacent strong $^{16}\text{OS}^{16}\text{O}$ (ν_1) and $^{18}\text{OS}^{18}\text{O}$ (ν_1) bands, respectively.

References. (1) Bennett et al. 2004; (2) Wan et al. 2009; (3) Zhou & Andrews 1999; (4) Bohn et al. 1992; (5) Bahou et al. 2000; (6) Jamieson et al. 2006; (7) Szczepanski et al. 1999; (8) Lo et al. 2004; (9) Garozzo et al. 2010; (10) Lugez et al. 2001; (11) Chaabouni et al. 2000; (12) Bennett & Kaiser 2005.

minutes yielding oxygen-rich ices with a composition of carbon disulfide to oxygen of 1 to 15 ± 1 and a total thickness of 175 ± 10 nm. To confirm the infrared assignments of the newly formed products, we also replaced $^{16}\text{O}_2$ by $^{18}\text{O}_2$ (Cambridge Isotope Laboratories Inc., 97%) and $^{16}\text{O}_2/^{18}\text{O}_2$ (1:1) gas mixtures. After the deposition, the infrared spectrum of each ice was recorded in absorption–reflection–absorption mode (reflection angle $\alpha = 75^\circ$) with a resolution of 4 cm^{-1} (Nicolet 6700 FTIR). Figure 1 depicts the mid-infrared spectra of a carbon disulfide–oxygen ice at 12 K. The vibrational frequencies are compiled in Table 1 along with their assignments. These ices were then irradiated isothermally at 12 K with 5 keV electrons generated by an electron gun (SPECS; EQ 22/35) at a nominal beam current of 0 nA (blank), 100 nA, 1000 nA, and 5000 nA over an area of $3.0 \pm 0.2 \text{ cm}^2$. Note that the actual extraction efficiency of the electron gun was stated to be 78.8%, which led to a corrected fluence of 5.5×10^{14} electrons cm^{-2} at a nominal current of 100 nA over 60 minutes. The radiation-induced chemical processing of the ices was monitored online and in situ by a Nicolet Infrared Spectrometer in a spectral range of 6000 to 400 cm^{-1} . After the completion of the irradiation, the ices were

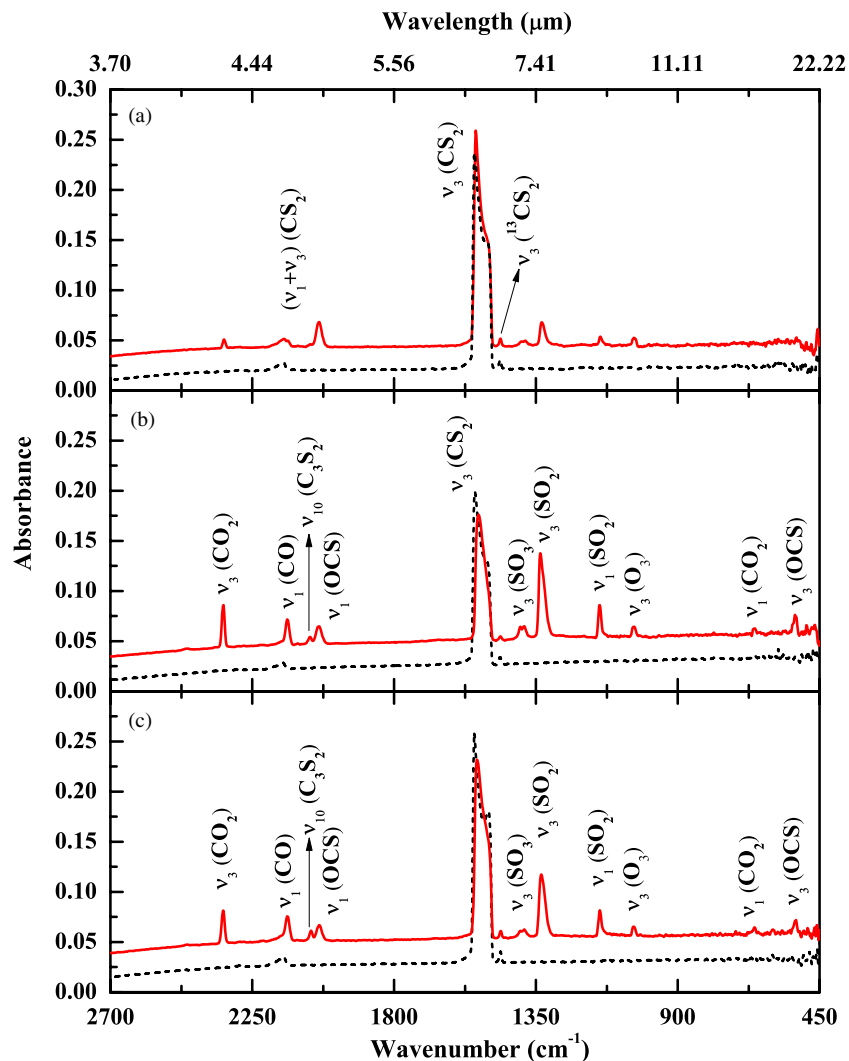


Figure 1. Infrared spectra of carbon disulfide (CS_2)–oxygen (O_2) ices at 12 K before irradiation (dashed trace) and after irradiation (solid trace) at three different currents of the electron beam: (A) 100 nA (3 hr) (B) 1000 nA (1 hr) and (C) 5000 nA (1 hr).

(A color version of this figure is available in the online journal.)

kept isothermally for 60 minutes before being heated to 300 K with a gradient of $0.5 \text{ K minute}^{-1}$.

3. RESULTS

First, we investigate the formation of new molecules during the irradiation at 12 K. Figure 1 depicts the infrared spectra of the ices recorded at 12 K before and after the irradiation at 100 nA (3 hr), 1000 nA (1 hr), and 5000 nA (1 hr). The new absorption features are compiled in Table 1 along with their assignments. The absorptions of carbon dioxide (CO_2) arose at 2342 cm^{-1} and 657 cm^{-1} ; these bands were assigned to the ν_3 and ν_1 fundamentals, respectively, and are in excellent agreement with the literature values of 2342 cm^{-1} and 658 cm^{-1} , respectively (Bennett et al. 2004; Garozzo et al. 2010). The ν_1 fundamental mode of carbon monoxide (CO) was detected at 2139 cm^{-1} (Bennett et al. 2004). The formation of carbonyl sulfide (OCS) was confirmed via the detection of ν_1 fundamental at 2039 cm^{-1} ; this data is in close agreement with the literature value of 2049 cm^{-1} (Garozzo et al. 2010; Lo et al. 2004). The doublets at 1399 cm^{-1} and 1388 cm^{-1} were identified as the ν_3 fundamental of sulfur trioxide (SO_3) and its dimer ($\text{SO}_3:\text{SO}_3$) (Garozzo et al. 2010;

Lo et al. 2004), respectively. Absorption of the sulfur dioxide (SO_2) fundamentals were probed at 1335 cm^{-1} (ν_3), 1148 cm^{-1} (ν_1), and 528 cm^{-1} (ν_2) with excellent correlation with literature values at 1337 cm^{-1} , 1150 cm^{-1} , and 520 cm^{-1} , respectively (Garozzo et al. 2010; Lo et al. 2004). The ν_3 fundamental of ozone (O_3) was detected at 1040 cm^{-1} (Bennett et al. 2004; Garozzo et al. 2010). Note that carbon monosulfide (CS) and sulfur monoxide (SO) were supposed to be observed around 1270 cm^{-1} and 1137 cm^{-1} , respectively, but no absorption features could be identified. This may be possibly due to the lower yield, the higher reactivity, and/or the proximity of the strong ν_3 and ν_1 absorption bands of sulfur dioxide (SO_2). At higher currents of 1000 nA and 5000 nA, the formation of carbon subsulfide (C_3S_2) was confirmed via the detection of the ν_{10} band at 2068 cm^{-1} (Szczepanski et al. 1999). The observation of C_3S_2 suggests the formation of carbon monosulfide (CS) in the irradiated ices, as polymerization of carbon monosulfide was implied in the formation of carbon subsulfide (C_3S_2 ; Cataldo 2006).

To confirm the assignments of the newly formed molecules, we also investigated the irradiation induced chemistry in isotopically labeled ices. The $\text{CS}_2\text{-}^{18}\text{O}_2$ and $\text{CS}_2\text{-}^{16}\text{O}_2\text{-}^{18}\text{O}_2$ ices (1:7.5:7.5) were irradiated at 1000 nA for 1 hr at 12 K. Selected

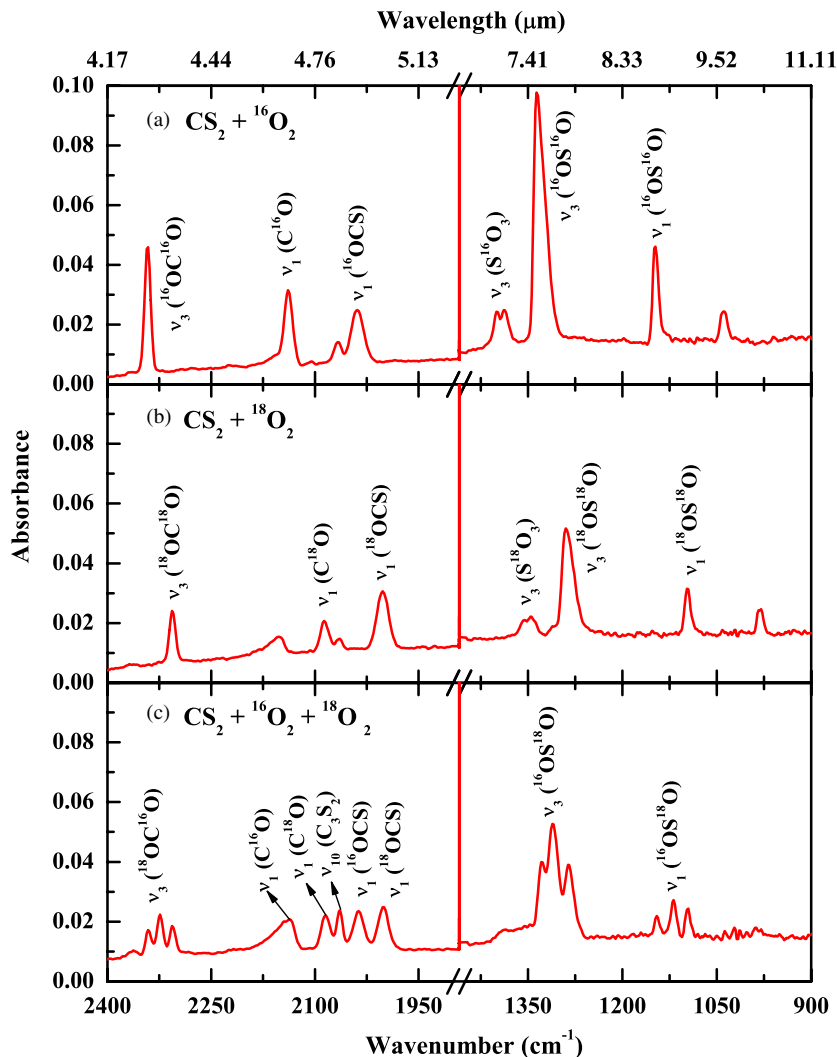


Figure 2. Infrared spectra of (A) carbon disulfide (CS_2) + $^{16}\text{O}_2$ (1:15) ices, (B) carbon disulfide (CS_2) + $^{18}\text{O}_2$ ices, and (C) carbon disulfide (CS_2) + $^{16}\text{O}_2$ + $^{18}\text{O}_2$ ices after irradiation at 1000 nA of the electron beam (1 hr) at 12 K.

(A color version of this figure is available in the online journal.)

regions of the infrared spectra from 900 cm^{-1} to 2400 cm^{-1} are depicted in Figure 2 along with the unlabeled ices (CS_2 - $^{16}\text{O}_2$) for comparison. The ^{18}O -bearing molecules were well separated from the ^{16}O -bearing species as depicted in Figures 2(A) and (B); the infrared spectra of the irradiated CS_2 - $^{16}\text{O}_2$ - $^{18}\text{O}_2$ ices clearly depicted the ^{16}O - and ^{18}O -bearing species along with three absorptions at 2324 cm^{-1} , 1312 cm^{-1} , and 1120 cm^{-1} , a broad absorption feature at 1400 – 1345 cm^{-1} region, and multiple transitions in the 1037 – 983 cm^{-1} region. The bands at 2324 cm^{-1} , 1312 cm^{-1} , and 1120 cm^{-1} could be easily assigned to the ν_3 fundamental of $^{16}\text{OC}^{18}\text{O}$ (Wan et al. 2009), to the ν_3 fundamental of $^{16}\text{OS}^{18}\text{O}$, and to the ν_1 fundamental of $^{16}\text{OS}^{18}\text{O}$ (Chaabouni et al. 2000), respectively. The broad absorption feature in the 1400 – 1345 cm^{-1} region and multiple bands in the 1037 – 983 cm^{-1} range were attributed to isotopologues of sulfur trioxide (SO_3 ; Chaabouni et al. 2000) and ozone (O_3 ; Sivaraman et al. 2010), respectively. It is important to note that as a result of the reaction of atomic oxygen (O) with carbon disulfide (CS_2) in low temperature argon matrices, Lo et al. (2004) confirmed the detection of OSCS and $\text{O}(\text{CS}_2)$. The presence of these isomers was also confirmed via quantum mechanical calculation by Cheng et al. (2001) and Lo et al. (2004). The C=S stretching vibration (ν_1) of $^{16}\text{OSCS}$ was observed at 1402 cm^{-1} (Lo et al.

2004); as expected, its $^{18}\text{OSCS}$ counterpart did not show any isotopic shift. In our work, the absorption features at 1399 cm^{-1} (Figure 1, Table 1) were assigned to SO_3 : SO_3 (ν_3); this was the only absorption close to the ν_1 vibration of $^{16}\text{OSCS}$. However, in the CS_2 - $^{18}\text{O}_2$ system, the absorption underwent a 41 cm^{-1} isotopic shift (Table 1; Figure 2); no absorption could be identified around 1400 cm^{-1} , confirming that no OSCS molecule was formed in our experiments within the detection limits. Furthermore, the ν_1 vibrational band of $\text{O}(\text{CS}_2)$ was observed at 1825 cm^{-1} by Lo et al. (2004). In our experiments, no absorption feature could be identified in this region.

4. DISCUSSION

Having identified the newly formed molecules qualitatively (Table 1; Figures 1 and 2), we are now focusing our attention on elucidating the possible reaction mechanisms and rate of formation of these species. For this purpose, a kinetic scheme was developed (Figure 3) to fit the column densities of the newly formed molecules during the irradiation at 100 nA (Figure 4). The column densities of the newly formed molecules along with carbon disulfide were determined by utilizing a modified Lambert-Beer relationship derived by Bennett et al. (2004). The

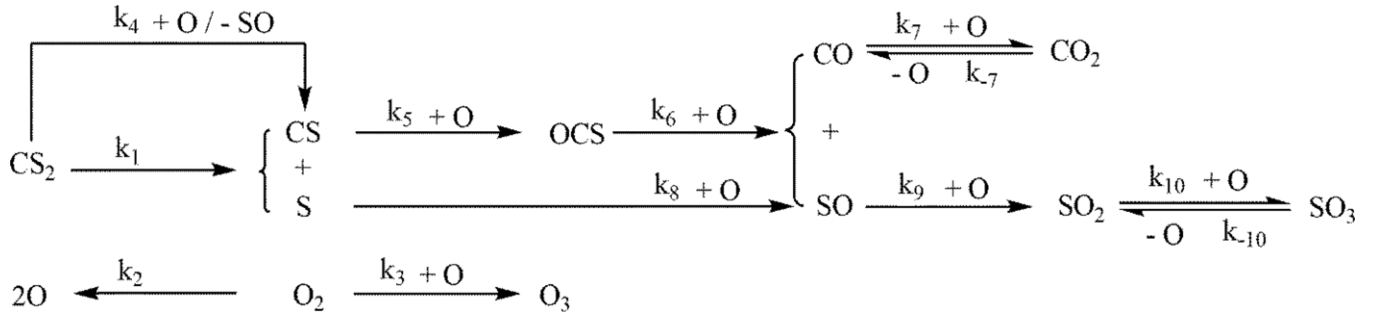


Figure 3. Reaction scheme used to fit the temporal profiles of the newly formed molecules in carbon disulfide (CS₂)–oxygen (O₂) ices at 12 K.

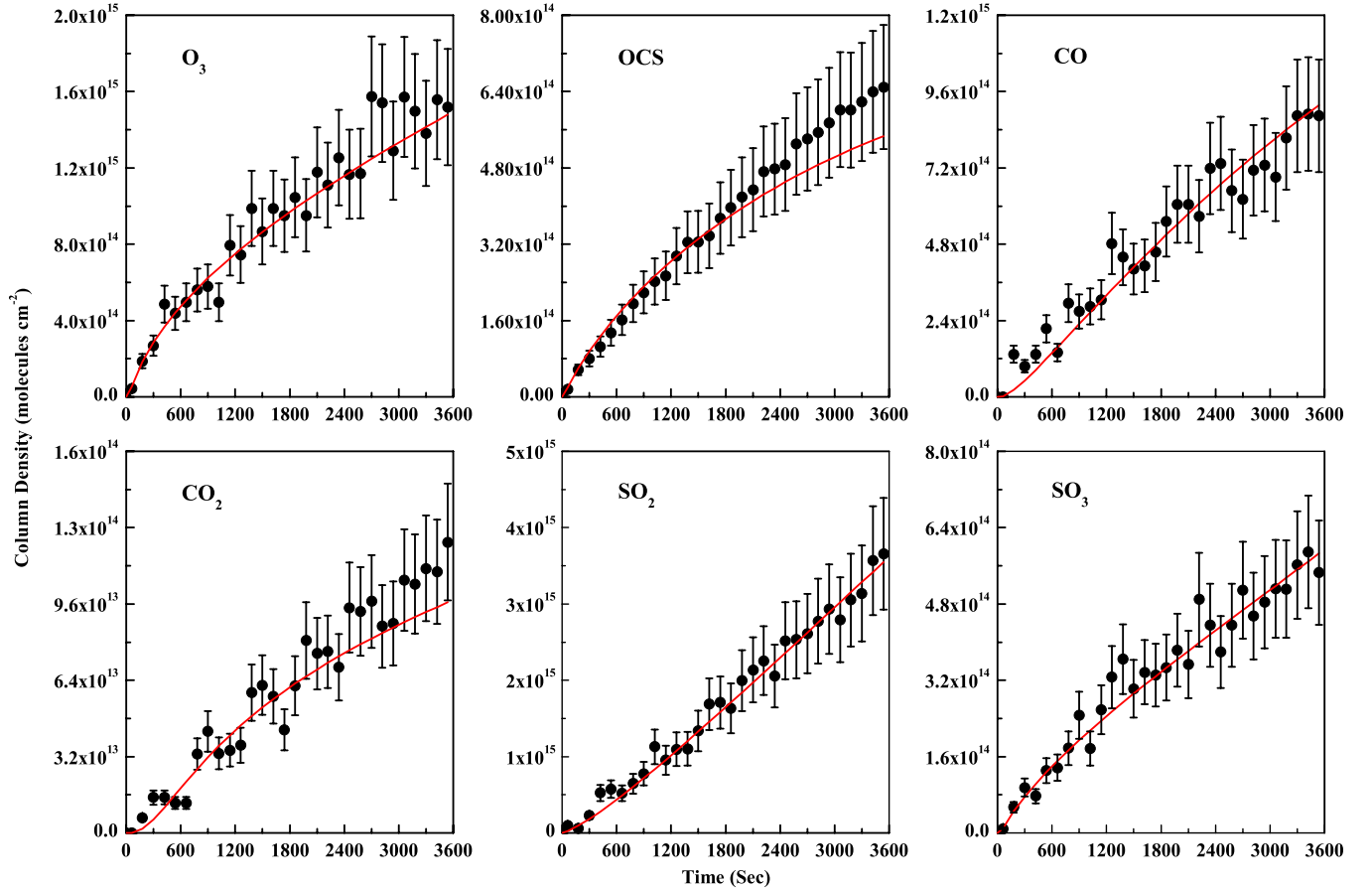


Figure 4. Fit of the column densities of ozone (O₃), carbonyl sulfide (OCS), carbon monoxide (CO), carbon dioxide (CO₂), sulfur dioxide (SO₂), and sulfur trioxide (SO₃) produced during the electron irradiation (100 nA) of carbon disulfide (CS₂)–oxygen (O₂) ices at 12 K.

(A color version of this figure is available in the online journal.)

integrated absorption coefficients used to calculate the column densities are listed in Table 2. A system of 12 coupled differential equations was solved numerically to fit the temporal evolution of the column densities of the emerging species during the radiation exposure (Frenklach et al. 1992). After 1 hr of irradiation, the carbon disulfide column density monitored via the absorption at 1525 cm⁻¹ decreased from $2.9 \pm 0.1 \times 10^{16}$ molecules cm⁻² to $2.6 \pm 0.1 \times 10^{16}$ molecules cm⁻² by about 10%. Considering the flux of 5.5×10^{14} electrons cm⁻² at 100 nA, each electron leads to the destruction of 20 ± 10 molecules of carbon disulfide.

Here, the experimental results (Figures 3 and 4) suggest that upon electron irradiation, the carbon disulfide (CS₂) molecule undergoes unimolecular decomposition to carbon monosulfide

(CS) and atomic sulfur (S) (R1). An analogous reaction mechanism was proposed previously to be the primary dissociation channel of carbon disulfide upon microwave discharge and high frequency discharge in an argon matrix (Bohn et al. 1992; Ma et al. 2009). The dissociation of carbon disulfide to both ground state carbon monosulfide, CS(*X*¹Σ⁺) and atomic sulfur, S(³P), is endoergic by 441 kJ mol⁻¹ (4.57 eV) (Table 3). The energy for this endoergic process can be supplied by the energy loss from electrons passing through the ice with an average linear energy transfer of 8.0 ± 1.0 keV μm⁻¹. Here, the rate constant of reaction (R1) was found to be $k_1 = 2.49 \pm 0.05 \times 10^{-5}$ s⁻¹ at 100 nA.

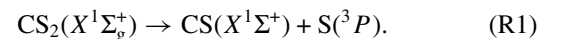
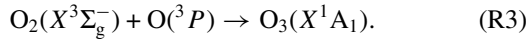
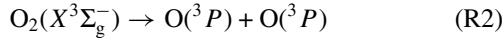


Table 2
Integrated Absorption Coefficients (*A*) Used in this Work

Molecule	Absorption (cm^{-1})	<i>A</i> (cm molecule^{-1})	Reference
CO ₂	2342	7.6×10^{-17}	1
CO	2139	1.1×10^{-17}	1
OCS	2049	1.5×10^{-16}	1
CS ₂	1524	9.1×10^{-17}	1
SO ₃	1385	3.0×10^{-17}	2
SO ₂	1352	1.5×10^{-17}	1
O ₃	1037	1.4×10^{-17}	1

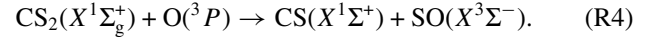
References. (1) Garozzo et al. 2010; (2) Majkowski et al. 1978.

However, we were unable to isolate the infrared absorption feature of carbon monosulfide (CS) around 1270 cm^{-1} . What might be the reason for this? We have to keep in mind that the carbon monosulfide molecules are formed within an oxygen-rich ice. Here, the interaction of the energetic electrons with the oxygen molecules can lead to homolytic bond cleavage, resulting in the formation of two oxygen atoms (R2). This reaction mechanism was proposed previously by Bennett & Kaiser (2005). This process is endoergic by 498 kJ mol^{-1} (5.17 eV). These oxygen atoms can react with molecular oxygen to form ozone, as detected in our experiment, via reaction (R3) with a rate of $k_3 = 4.72 \pm 0.50 \times 10^{-20} \text{ cm}^2 \text{ molecule}^{-1} \text{ s}^{-1}$. It is important to note that the nascent oxygen atoms released in reaction (R2) can carry an excess kinetic energy of up to a few electron volt, which can facilitate the easy escape of the oxygen atom from the matrix cage (Bennett & Kaiser 2005).

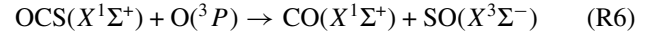


Our kinetics scheme further proposes that the reaction of carbon disulfide (CS₂) with suprathemal atomic oxygen (O) can lead to the formation of carbon monosulfide (CS) and sulfur monoxide (SO), reaction (R4), via the ‘‘pickup’’ of a sulfur atom by the suprathemal oxygen atom. This mechanism was also identified as the major reaction pathway with fractions of up to

90% in the crossed molecular beam investigation of O(³P) with CS₂ (Rochford et al. 1995), via the gas phase reaction of CS₂ and nascent oxygen (O) produced via the photolysis of nitrogen dioxide (NO₂) (Cheng et al. 2001), and in the reaction between CS₂ and nascent oxygen (O) produced via the photolysis of ozone (O₃) in an argon matrix (Lo et al. 2004):



Now we turn our attention toward the formation of carbonyl sulfide (OCS). Reaction (R5) depicts the formation of the latter via the addition of atomic oxygen to carbon monosulfide (CS). The analogous reaction (R5) was suggested to present the primary reaction channel to the formation of carbonyl sulfide (OCS) in the interstellar medium (Palumbo et al. 1997; Ward et al. 2012) in the presence of carbon monosulfide (CS). Note that both reactions (R4) and (R5) are exoergic (Table 3). The rate constants of reactions (R4) and (R5) were determined to be $k_4 = 1.10 \pm 1.00 \times 10^{-22} \text{ cm}^2 \text{ molecule}^{-1} \text{ s}^{-1}$ and $k_5 = 3.08 \pm 1.00 \times 10^{-16} \text{ cm}^2 \text{ molecule}^{-1} \text{ s}^{-1}$, respectively. Therefore, the non-detection of carbon monosulfide formed in reaction (R1) is likely the result of a rapid reaction of the latter with atomic oxygen via reaction (R5):



To fit the temporal profile of carbonyl sulfide (OCS), we had to include a destruction pathway reaction (R6) with a rate of $k_6 = 8.79 \pm 0.80 \times 10^{-17} \text{ cm}^2 \text{ molecule}^{-1} \text{ s}^{-1}$. This channel was proposed previously (Froese & Goddard 1993; Palumbo et al. 1997; Rochford et al. 1995). Eventually, carbon monoxide (CO) can react with energetic oxygen atoms to yield carbon dioxide (CO₂) via reaction (R7). The addition of an oxygen atom (O) to carbon monoxide (CO) yielding carbon dioxide (CO₂) (R7) can also support the observed yields of the carbon dioxide isotopologues (¹⁶OC¹⁶O, ¹⁶OC¹⁸O, ¹⁸OC¹⁸O) of 1:2:1.

Table 3
Rate Constants Derived via Iterative Solution of the Reaction Scheme in Figure 3 Along with Reaction Energies

	Rate Constant ^a	Reactions	$\Delta_R G^b$	
			(kJ mol^{-1})	(eV)
k_1	$2.49 \pm 0.05 \times 10^{-5}$	$\text{CS}_2(X^1\Sigma_g^+) \rightarrow \text{CS}(X^1\Sigma^+) + \text{S}({}^3P)$	440.5	4.57
k_2	$4.22 \pm 0.10 \times 10^{-6}$	$\text{O}_2(X^3\Sigma_g^-) \rightarrow \text{O}({}^3P) + \text{O}({}^3P)$	498.4	5.17
k_3	$4.72 \pm 0.50 \times 10^{-20}$	$\text{O}_2(X^3\Sigma_g^-) + \text{O}({}^3P) \rightarrow \text{O}_3(X^1A_1)$	-106.5	-1.10
k_4	$1.10 \pm 1.00 \times 10^{-22}$	$\text{CS}_2(X^1\Sigma_g^+) + \text{O}({}^3P) \rightarrow \text{CS}(X^1\Sigma^+) + \text{SO}(X^3\Sigma^-)$	-80.9	-0.84
k_5	$3.08 \pm 1.00 \times 10^{-16}$	$\text{CS}(X^1\Sigma^+) + \text{O}({}^3P) \rightarrow \text{OCS}(X^1\Sigma^+)$	-667.9	-6.92
k_6	$8.79 \pm 0.80 \times 10^{-17}$	$\text{OCS}(X^1\Sigma^+) + \text{O}({}^3P) \rightarrow \text{CO}(X^1\Sigma^+) + \text{SO}(X^3\Sigma^-)$	-216.3	-2.24
k_7	$3.20 \pm 0.90 \times 10^{-17}$	$\text{CO}(X^1\Sigma^+) + \text{O}({}^3P) \rightarrow \text{CO}_2(X^1\Sigma_g^+)$	-532.2	-5.52
k_{-7}	$3.87 \pm 0.40 \times 10^{-3}$	$\text{CO}_2(X^1\Sigma_g^+) \rightarrow \text{CO}(X^1\Sigma^+) + \text{O}({}^3P)$	532.2	5.52
k_8	$3.28 \pm 1.00 \times 10^{-13}$	$\text{S}({}^3P) + \text{O}({}^3P) \rightarrow \text{SO}(X^3\Sigma^-)$	-521.4	-5.40
k_9	$1.58 \pm 1.00 \times 10^{-15}$	$\text{SO}(X^3\Sigma^-) + \text{O}({}^3P) \rightarrow \text{SO}_2(X^1A_1)$	-651.0	-6.75
k_{10}	$3.85 \pm 0.50 \times 10^{-16}$	$\text{SO}_2(X^1A_1) + \text{O}({}^3P) \rightarrow \text{SO}_3(X^1A_1')$	-248.2	-2.75
k_{-10}	$3.08 \pm 0.50 \times 10^{-2}$	$\text{SO}_3(X^1A_1') \rightarrow \text{SO}_2(X^1A_1) + \text{O}({}^3P)$	248.2	2.75

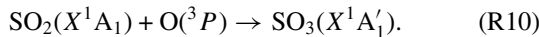
Notes. The uncertainties in rate constants represent the acceptable limits of the fit within the error limits of the column densities.

^a Units in s^{-1} for k_1 , k_2 , k_{-7} and k_{-10} (first order) and in $\text{cm}^2 \text{ molecule}^{-1} \text{ s}^{-1}$ (second order) for others.

^b Derived from NIST database.

Induced by energetic electrons, the carbon dioxide formed in reaction (R7) can also dissociate back to carbon monoxide and atomic oxygen (O) (Bennett et al. 2004). The rates of formation and dissociation were calculated to be $k_7 = 3.20 \pm 0.90 \times 10^{-17} \text{ cm}^2 \text{ molecule}^{-1} \text{ s}^{-1}$ and $k_{-7} = 3.87 \pm 0.40 \times 10^{-3} \text{ s}^{-1}$, respectively.

Finally, we would like to discuss the formation of the sulfur oxides in the irradiated ices. Besides the formation of sulfur monoxide via reactions (R4) and (R6), the atomic sulfur (S) produced in reaction (R1) can promptly react with an energetic oxygen atom (O) to form SO (R8). The rate of oxygen addition to sulfur was calculated as fast as $k_8 = 3.28 \pm 1.00 \times 10^{-13} \text{ cm}^2 \text{ molecule}^{-1} \text{ s}^{-1}$. Furthermore, our kinetics scheme indicates that the stepwise addition of an oxygen atom to sulfur monoxide (SO) can lead to the formation of sulfur dioxide (SO₂) and sulfur trioxide (SO₃) via reactions (R9) and (R10):



Based on our isotope labeling, we observed a ratio of column densities of ¹⁶OS¹⁶O, ¹⁶OS¹⁸O, and ¹⁸OS¹⁸O species close to 1:2:1. The reaction pathway (R9) clearly supported the observed statistical ratio of sulfur dioxide isotopologues and confirmed that SO₂ was formed via the addition of an oxygen atom to the sulfur monoxide molecule. If the reaction proceeds via the reaction of molecular oxygen (O₂) with the sulfur (S) atom, then only ¹⁶OS¹⁶O and ¹⁸OS¹⁸O should have been detected; no ¹⁶OS¹⁸O should have been observable. The observation of ¹⁶OS¹⁸O indicates the involvement of sulfur monoxide in the formation of sulfur dioxide and sulfur trioxide. Here, the rate of formation of sulfur dioxide via the addition of an oxygen atom to sulfur monoxide was calculated to be $k_9 = 1.58 \pm 1.00 \times 10^{-15} \text{ cm}^2 \text{ molecule}^{-1} \text{ s}^{-1}$. Finally, the sulfur trioxide (SO₃) can also dissociate back to sulfur dioxide and atomic oxygen. The rate constants of the formation and dissociation of sulfur trioxide were calculated to be $k_{10} = 3.85 \pm 0.50 \times 10^{-16} \text{ cm}^2 \text{ molecule}^{-1} \text{ s}^{-1}$ and $k_{-10} = 3.08 \pm 0.50 \times 10^{-2} \text{ s}^{-1}$.

5. ASTROPHYSICAL IMPLICATION AND CONCLUSION

The present study demonstrates the formation of sulfur-bearing molecules, i.e., sulfur dioxide (SO₂), sulfur trioxide (SO₃), and carbonyl sulfide (OCS), in icy mixtures containing carbon disulfide (CS₂) when exposed to ionizing radiation in the form of energetic electrons. With the exception of SO₃, sulfur dioxide (SO₂) and carbonyl sulfide (OCS) were detected in the interstellar ices (Gibb et al. 2004). In this study, we have used oxygen (O₂) as a source of energetic oxygen atoms since the presence of condensed oxygen was predicted in interstellar ices (Bennett & Kaiser 2005). However, any oxygen-bearing molecules such as water (H₂O) (Zheng et al. 2006) and carbon dioxide (CO₂) (Bennett et al. 2004) can potentially act as a precursor to form atomic oxygen via the interaction of secondary electrons produced in the track of galactic cosmic ray particles (GCR) upon penetrating ices.

Gibb et al. (2004) confirmed the presence of sulfur dioxide (SO₂) and carbonyl sulfide (OCS) in the interstellar ices by investigating the *Infrared Space Observatory* (ISO) data of 23 infrared sources (YSOs). In the present study, both species were

produced during the electron irradiation on CS₂-O₂ ices. The previous kinetic models of the sulfur chemistry in the interstellar media (Prasad & Huntress 1982; Oppenheimer & Dalgarno 1974; Doty et al. 2002; Garrod et al. 2007; Millar & Herbst 1990; Wakelam et al. 2011) suggested that a significant amount of sulfur must be depleted on icy grain mantles. Except SO₂ and OCS, the chemical forms of sulfur in the interstellar ices are not yet fully known. However, the presence of CS₂ was proposed as a sulfur reservoir in the interstellar ices (Garozzo et al. 2010; Palumbo et al. 1997; Ward et al. 2012). Most importantly, the abundance of carbonyl sulfide (OCS) present in icy mantles is predominantly higher than the abundance in the gas phase of interstellar media (Palumbo et al. 1997), which clearly suggests that the formation of OCS in the interstellar media is mostly governed by an active grain chemistry rather than gas phase chemistry. Finally, since both of the sulfur-bearing molecules, OCS and SO₂, in the interstellar ices contain oxygen atoms, we propose that any CS₂ present in interstellar ices can react promptly with energetic oxygen atoms to form OCS and SO₂ in the presence of energetic GCR particles. Furthermore, our laboratory studies suggest that sulfur trioxide presents a likely target for future astronomical searches of molecules in interstellar ices.

S.M. wishes to thank Dr. Y. S. Kim for his support during the experiments. This work was supported by the Air Force Office of Scientific Research (FA9550-12-1-0213).

REFERENCES

- Bahou, M., Lee, Y.-C., & Lee, Y.-P. 2000, *JChS*, 122, 661
 Barker, E. S. 1979, *GeoRL*, 6, 117
 Bennett, C. J., Jamieson, C., Mebel, A. M., & Kaiser, R. I. 2004, *PCPP*, 6, 735
 Bennett, C. J., & Kaiser, R. I. 2005, *ApJ*, 635, 1362
 Bohn, R. B., Hannachi, Y., & Andrews, L. 1992, *JChS*, 114, 6452
 Boogert, A. C. A., Schutte, W. A., Helmich, F. P., Tielens, A., & Wooden, D. H. 1997, *A&A*, 317, 929
 Cataldo, F. 2006, *J. Inorg. Organomet. Polym.*, 16, 15
 Chaabouni, H., Schriver-Mazzuoli, L., & Schriver, A. 2000, *JPCA*, 104, 3498
 Cheng, Y., Han, J., Chen, X., Ishikawa, Y., & Weiner, B. R. 2001, *JPCA*, 105, 3693
 Doty, S. D., van-Dishoeck, E. F., van-der-Tak, F. F. S., & Boonman, A. M. S. 2002, *A&A*, 389, 446
 Ferrante, R. F., Moore, M. H., Spiliotis, M. M., & Hudson, R. L. 2008, *ApJ*, 684, 1210
 Frenklach, M., Wang, H., & Roabinowitch, M. J. 1992, *Prog. Energy Combust. Sci.*, 19, 47
 Froese, R. D. J., & Goddard, J. D. 1993, *MoPh*, 79, 685
 Garozzo, M., Fulvio, D., Kanuchova, Z., Palumbo, M. E., & Strazzulla, G. 2010, *A&A*, 509, A67
 Garrod, R. T., Wakelam, V., & Herbst, E. 2007, *A&A*, 467, 1103
 Geballe, T. R., Baas, F., Greenberg, J. M., & Schutte, W. 1985, *A&A*, 146, L6
 Gibb, E. L., Whittet, D. C. B., Boogert, A. C. A., & Tielens, A. G. G. M. 2004, *ApJS*, 151, 35
 Gottlieb, C. A., & Ball, J. A. 1973, *ApJL*, 184, L59
 Heynmann, D., Cataldo, F., Thiemens, M. H., Fokkens, R., Nibbering, N. M. M., & Vis, R. D. 2000, *M&PS*, 35, 355
 Jackson, W. M., Halpern, J. B., Feldman, P. D., & Rahe, J. 1982, *A&A*, 107, 385
 Jamieson, C. S., Mebel, A. M., & Kaiser, R. I. 2006, *APJS*, 163, 184
 Jefferts, K. B., Penzias, A. A., Wilson, R. W., & Solomon, P. M. 1971, *ApJL*, 168, L111
 Jones, P. R., & Taube, H. 1973, *JPhCh*, 77, 1007
 Lo, W. J., Chen, H. F., Chou, P. H., & Lee, Y. P. 2004, *JCP*, 121, 12371
 Lodders, K. 2003, *ApJ*, 591, 1220
 Lovas, F. J., & Dragoset, R. A. 2004, *JPCRD*, 33, 177
 Lugez, C. L., Thompson, W. E., & Jacox, M. E. 2001, *JPC*, 155, 166
 Ma, R., Yuan, D., Chen, M., et al. 2009, *JPCA*, 113, 4976
 Majkowski, R. F., Blint, R. J., & Hill, J. C. 1978, *ApOpt*, 17, 975

- Martin, S., Martin-Pintado, J., Mauersberger, R., Henkel, C., & Garcia-Burillo, S. 2005, *ApJ*, **620**, 210
- Millar, T. J., & Herbst, E. 1990, *A&A*, **231**, 466
- Oppenheimer, M., & Dalgarno, A. 1974, *ApJ*, **187**, 231
- Palumbo, M. E., Geballe, T. R., & Tielens, A. 1997, *ApJ*, **479**, 839
- Palumbo, M. E., Tielens, A., & Tokunaga, A. T. 1995, *ApJ*, **449**, 674
- Penzias, A. A., Solomon, P. M., Wilson, R. W., & Jefferts, K. B. 1971, *ApJL*, **168**, L53
- Prasad, S. S., & Huntress, W. T., Jr. 1982, *ApJ*, **260**, 590
- Rochford, J. J., Powell, L. J., & Grice, R. 1995, *J. Phys. Chem.*, **99**, 15369
- Sivaraman, B., Mebel, A. M., Mason, N. J., Babikov, D., & Kaiser, R. I. 2010, *PCCP*, **13**, 421
- Snyder, L. E., Hollis, J. M., Ulish, B. L., et al. 1975, *ApJL*, **198**, L81
- Sofia, U. J., Cardelli, J. A., & Savage, B. D. 1994, *ApJ*, **430**, 650
- Szczepanski, J., Hodyss, R., Fuller, J., & Vala, M. 1999, *JPCA*, **103**, 2975
- Thaddeus, P., Kutner, M. L., Penzias, A. A., Wilson, R. W., & Jefferts, K. B. 1972, *ApJL*, **176**, L73
- van Steenbergen, M. E., & Shull, J. M. 1988, *ApJ*, **330**, 942
- Wakelam, V., Hersant, F., & Herpin, F. 2011, *A&A*, **529**, A112
- Wan, L., Wu, L., Liu, A.-W., & HuC, S.-M. 2009, *JMoSp*, **257**, 217
- Ward, M. D., Hogg, I. A., & Price, S. D. 2012, *MNRAS*, **425**, 1264
- Williams, J. P., & Blitz, L. 1998, *ApJ*, **494**, 657
- Woods, P. M., Schoier, F. L., Nymman, L. A., & Olofsson, H. 2003, *A&A*, **402**, 617
- Zasowski, G., Kemper, F., Watson, D. M., et al. 2009, *ApJ*, **694**, 459
- Zheng, W., Jewitt, D., & Kaiser, R. I. 2006, *ApJ*, **639**, 534
- Zhou, M. F., & Andrews, L. 1999, *JCP*, **110**, 2414